IV. Conclusions

These results show that the LDAP-PW method can produce accurate structural parameters for molecules. The data suggest that the method which uses plane waves, pseudopotentials, and supercells may be a useful alternative to standard ab initio quantum-mechanical methods for calculations on chemical systems. Future work will include more realistic density functionals and tests of energetics of chemical transformations. In addition, research is continuing to develop more efficient energy minimization algorithms and superior pseudopotentials. These changes will improve the efficiency and accuracy of the method for the study of periodic and aperiodic chemical and biochemical systems.

Acknowledgment. This research was supported in part by the Florida State University Supercomputer Computations Research Institute, which is partially funded by the U.S. Department of Energy through Contract No. DE-FC05-85ER250000 and ONR Contract No. N00014-86-K-0158. We also acknowledge computer time provided by the Florida State University Computing Center, the MIT Supercomputer Facility, and the San Diego Supercomputer Center. One of us (A.M.R.) is supported by a Joint Services Electronics Program fellowship.

(35) Baughcum, S. L.; Duerst, R. W.; Rowe, W. F.; Smith, Z.; Wilson, E. B. *J. Am. Chem. Soc.* **1981**, *103*, 6296.

Ab Initio Prediction of the Structure and Stabilities of the Hypermagnesium Molecules: Mg_2O, Mg_3O, and Mg_4O

Alexander I. Boldyrev,[†,‡] Igor L. Shamovsky,[‡] and Paul von R. Schleyer*,[†]

Contribution from the Institut für Organische Chemie, Friedrich-Alexander Universität Erlangen-Nürnberg, Henkestrasse 42, 8520 Erlangen, FRG, and Institute of Chemical Physics of the Russian Academy of Sciences, Kosygin Street 4, 117334 Moscow, Russia.
Received August 21, 1991

Abstract: The concept of hypermetalation, characterized by molecules with unprecedented stoichiometries, is extended to the magnesium–oxygen combinations, Mg_2O, Mg_3O, and Mg_4O. Their equilibrium geometries and fundamental frequencies were calculated at the HF/6-31G* and correlated MP2 (full)/6-31G* levels. Extensive searches of possible structures and electronic states were carried out. The global minima are as follows: linear Mg_2O ($D_{\infty h}$, both singlet $^1\Sigma_g^+$ and the triplet $^3\Sigma_u^-$ states), planar Mg_3O (D_{3h}, $^3A_1'$), and Mg_4O forms slightly distorted from the square planar arrangement (D_{2d}, $^1A_1$ and planar $MgOMg_3$ (C_s, $^1A_1$) structures have nearly the same energy). These Mg_2O, Mg_3O, and Mg_4O species are stable with regard to all possible decomposition pathways. Representative dissociation energies are the following: Mg_2O, 74.5 kcal/mol into MgO + Mg at QCISD (T)/6-311+G(3df)+ZPE; Mg_3O, 26.7 kcal/mol into Mg_2O + Mg at QCISD(T)/6-311+G*+ZPE; and Mg_4O, 7.9 kcal/mol into Mg_3O + Mg at MP4SDTQ/6-311+G*+ZPE. Magnesium–magnesium bonding contributes significantly to the stability of Mg_3O and Mg_4O.

Introduction

Hypermetalation, involving metal stoichiometries exceeding normal valence expectations, should be a general phenomenon exhibited by many if not all metals. Hyperalkali metal molecules are now well-documented. Many hyperlithium molecules, OLi_4, OLi_5, OLi_6, NLi_5, CLi_5, OLi_6, BLi_5, $BeLi_4$, $BeLi_4$, $BeLi_6$, etc., were discovered by calculation.[1-9] Li_3O, Li_4O, and Li_5O have been observed by mass spectrometry and atomization energies determined.[10,11] There is similar evidence for Na_2Cl,[12] Na_3O, Na_4O, K_3O, K_4O,[13,14] and Cs_8O.[15] The "suboxides" of rubidium and cesium, e.g., Rb_2O_2, Cs_7O, and $Cs_{11}O_3$, have been characterized.[16,17] Bonding interactions between ligand atoms contribute to both the structure and the stability of these species.[1-9] Despite having the usual stoichiometry, $SiLi_4$ also is instructive. Metal–metal bonding contributes to the surprising preference for a

[†] Universität Erlangen-Nürnberg.
[‡] Russian Academy of Sciences.

(1) Schleyer, P. v. R.; Wurthwein, E.-U.; Pople, J. A. *J. Am. Chem. Soc.* **1982**, *104*, 5839.
(2) Schleyer, P. v. R. In *New Horizons of Quantum Chemistry*; Lowdin, P.-O., Pullman, A., Eds.; Reidel: Dordrecht, The Netherlands, 1983; pp 95–105.
(3) Schleyer, P. v. R.; Wuthwein, E.-U.; Kaufmann, E.; Clark, T. *J. Am. Chem. Soc.* **1983**, *105*, 5930.
(4) Gutsev, G. L.; Boldyrev, A. I. *Chem. Phys. Lett.* **1982**, *92*, 262.
(5) Pewestorf, W.; Bonacic-Koutecky, V.; Koutecky, J. *J. Chem. Phys.* **1988**, *89*, 5794,
(6) Fantucci, P.; Bonacic-Koutecky, V.; Pewestorf, W.; Koutecky, J. *J. Chem. Phys.* **1989**, *91*, 4229.
(7) Klimenko, N. M.; Musaev, D. G.; Gorbik, A. A.; Zyubin, A. S.; Charkin, O. P.; Wurthwein, E.-U.; Schleyer, P. v. R. *Koord. Khim.* **1986**, *12*, 601 (in Russian).
(8) Schleyer, P. v. R. *Pure Appl. Chem.* **1984**, *56*, 151.
(9) Savin, A.; Preuss, H.; Stoll, H. *Rev. Roum. Chim.* **1987**, *32*, 1069.

0002-7863/92/1514-6469$03.00/0

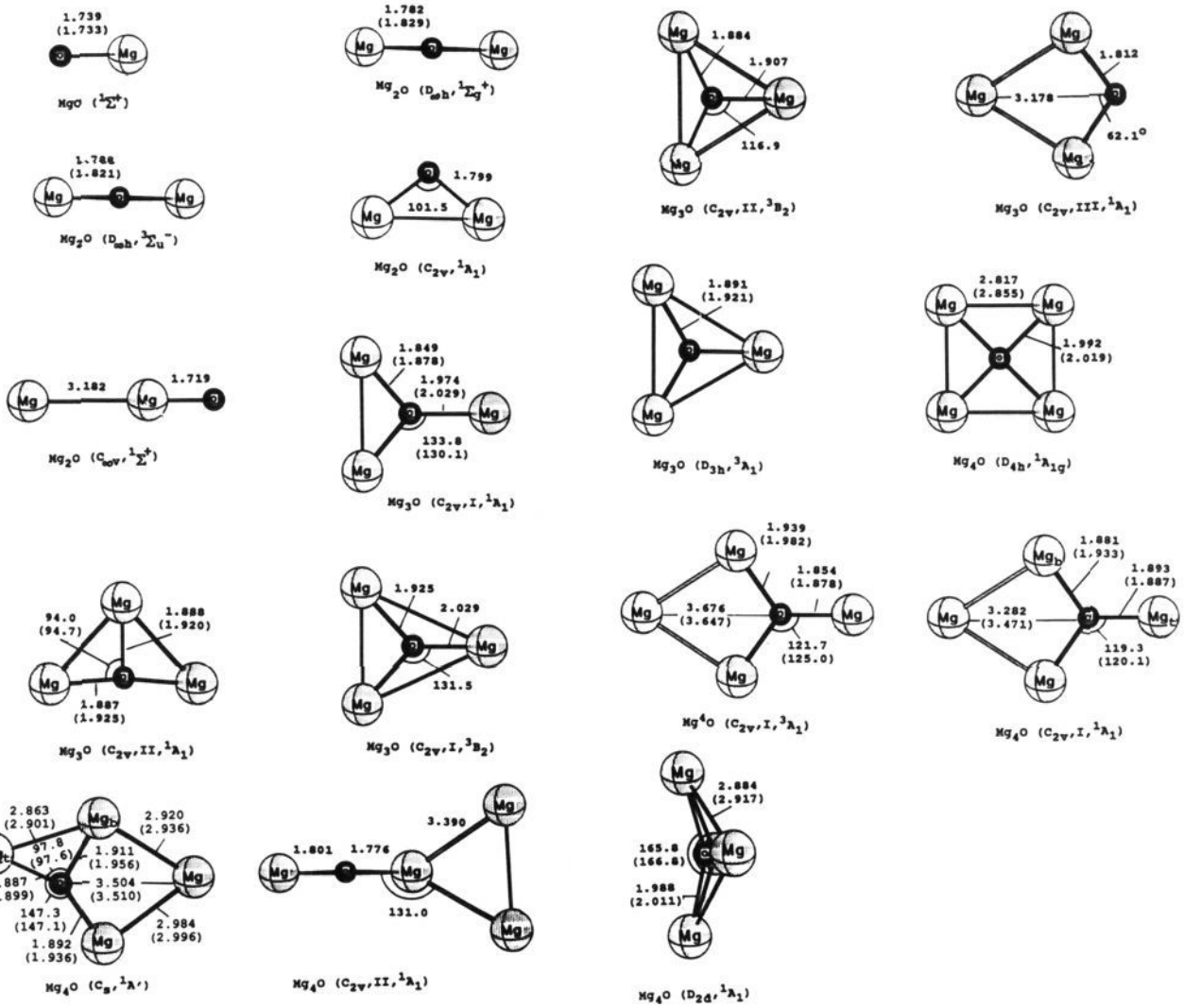

Figure 1. Optimized geometries of the magnesium oxides (bond length in Å and valence angles in deg). Geometries at MP2(full)/6-31G* are given in parentheses. Other data at HF/6-31G*.

nontetrahedral, C_{2v} point group geometry.[18,19] We have recently investigated the hyperaluminum molecules, Al_3O and Al_4O, computationally:[20] planar Al_3O (the C_{2v}, Y-shaped ($^2A_1$) and T-shaped ($^2B_2$) forms have nearly the same energy) and planar Al_4O (D_{4h}, $^1A_{1g}$) structures were predicted to be the global minima. Both of these species are very stable with regard to all possible decomposition pathways. There also is mass spectrometric evidence for Al_3O.[21]

We have now extended our ab initio investigations to the hypermagnesium molecules, Mg_2O, Mg_3O, and Mg_4O. While experimental and theoretical studies of the MgO monomer are extensive,[22-32] we have not been able to find any information on the isolated Mg_2O, Mg_3O, and Mg_4O molecules. However, Mg_4O and Mg_6O clusters as models for oxygen chemosorption on metal magnesium surfaces were examined,[33,34] but full optimization of the geometries and characterization via frequency calculations were not carried out. Hypermagnesium RMg_nHal molecules containing linear –Mg–Mg–Mg– chains have been studied.[35] However, the extra Mg atoms are bound in these molecules by only 2 kcal/mol (6 kcal/mol when $n = 2$).

Computational Methods

Geometries of MgO, Mg_2O, Mg_3O, and Mg_4O were optimized employing analytical gradients[36] with a polarized split-valence basis

(10) Wu, C. H.; Kudo, H.; Ihle, H. R. *J. Chem. Phys.* **1979**, *70*, 1815.
(11) Wu, C. H. *Chem. Phys. Lett.* **1987**, *139*, 357.
(12) Peterson, K. I.; Dao, P. D.; Castleman, A. W., Jr. *J. Chem. Phys.* **1983**, *79*, 777.
(13) Dao, P. D.; Peterson, K. I.; Castleman, A. W., Jr. *J. Chem. Phys.* **1984**, *80*, 563.
(14) Wurthwein, E.-U.; Schleyer, P. v. R.; Pople, J. A. *J. Am. Chem. Soc.* **1984**, *106*, 6973.
(15) Fallgren, H.; Martin, T. P. *Chem. Phys. Lett.* **1990**, *168*, 233.
(16) Simson, A. *Bonding (Berlin)* **1979**, *36*, 81.
(17) Borgstedt, H. V. *Top. Curr. Chem.* **1986**, *134*, 125.
(18) Schleyer, P. v. R.; Reed, A. E. *J. Am. Chem. Soc.* **1988**, *110*, 4453.
(19) Reed, A. E.; Schleyer, P. v. R.; Janoschek, R. *J. Am. Chem. Soc.* **1991**, *113*, 1885.
(20) (a) Boldyrev, A. I.; Schleyer, P. v. R. *J. Am. Chem. Soc.* **1991**, *113*, 9045. (b) Schleyer, P. v. R.; Boldyrev, A. I. *J. Chem. Soc., Chem. Commun.* **1991**, 1536.
(21) Cox, D. M.; Trevor, D. J.; Whetten, R. L.; Rohlfing, E. A.; Kaldor, A. *J. Chem. Phys.* **1986**, *84*, 4651.
(22) Liu, B.; Olson, R. E.; Saxon, R. P. *J. Chem. Phys.* **1981**, *74*, 4216.
(23) Meyer, W.; Rosmus, P. *J. Chem. Phys.* **1981**, *74*, 4217.
(24) Bauschlicher, C. W., Jr.; Lengsfield, B. H., III; Liu, B. *J. Chem. Phys.* **1982**, *77*, 4084.
(25) Langhoff, S. R.; Bauschlicher, C. W., Jr.; Partidge, H. *J. Chem. Phys.* **1986**, *84*, 4474.
(26) Veits, I. V.; Gurvich, G. V. *Zh. Fiz. Khim.* **1957**, *31*, 2306.
(27) Drowart, J.; Exsteen, G.; Verhaegen, G. *Trans. Faraday Soc.* **1964**, *60*, 1920.
(28) Cotton, D. H.; Yenkins, D. R. *Trans. Faraday Soc.* **1969**, *65*, 376.
(29) Zeegers, P. J. I.; Townsend, W. P.; Winefordner, J. D. *Spectrochim. Acta, Part B* **1969**, *26*, 234.
(30) Farber, M.; Srivastava, R. D. *High Temp. Sci.* **1976**, *8*, 195.
(31) Srivastava, R. D. *High. Temp. Sci.* **1976**, *8*, 225.
(32) Ikeda, T.; Wong, N. B.; Harris, D. O.; Field, R. W. *J. Mol. Spectrosc.* **1977**, *68*, 452.
(33) Sakoto, C. *Phys. Rev.* **1984**, *B30*, 1754.
(34) Broughton, J. Q.; Bagus, P. S. *Phys. Rev.* **1987**, *112*, 2813.
(35) Jasien, P. G.; Dykstra, C. E. *J. Am. Chem. Soc.* **1985**, *107*, 1891.

Table I. Calculated Total (E_{tot}) and Relative (ΔE) Energies of Magnesium Oxide Species[a]

species	$\langle S^2 \rangle$	E_{tot}, au	ΔE, kcal/mol
Mg(S)	0	−199.595 61	
O(3p)	2.006	−74.783 93	
$MgO(^1\Sigma^+)$	0	−274.323 83	
$Mg_2O(D_{\infty h}, {}^3\Sigma_u^-)$	2.002	−474.101 72 (0)	0.0
$Mg_2O(C_{2v}, {}^1A_1)$	0	−474.029 55 (0)	45.3
$Mg_2O(D_{\infty h}, {}^1\Sigma_g^+)$	0	−474.027 97 (2)	46.3
$Mg_2O(C_{\infty v}, {}^1\Sigma^+)$	0	−473.932 11 (0)	106.4
$Mg_3O(C_{2v}, I({}^3B_2))$	2.362	−673.732 20 (0)	0.0
$Mg_3O(D_{3h}, {}^3A_1)$	2.130	−673.727 37 (2)	3.0
$Mg_3O(C_{2v}, II({}^1A_1))$	0	−673.677 66 (0)	34.2
$Mg_3O(C_{2v}, I({}^1A_1))$	0	−673.664 79 (0)	42.3
$Mg_3O(C_{2v}, III({}^1A_1))$	0	−673.645 86 (0)	54.2
$Mg_4O(C_{2v}, I({}^3A_1))$	2.749	−873.325 45 (0)	0.0
$Mg_4O(C_s, {}^1A')$	0	−873.293 32 (0)	20.2
$Mg_4O(C_{2v}, I({}^1A_1))$	0	−873.290 56 (1)	21.9
$Mg_4O(D_{2d}, {}^1A_1)$	0	−873.283 70 (0)	26.2
$Mg_4O(D_{4h}, {}^1A_{1g})$	0	−873.281 41 (1)	27.7
$Mg_4O(C_{3v}, I({}^1A_1))$	0	−873.257 42	42.7
$Mg_4O(C_{2v}, II({}^1A_1))$	0	−873.228 59	60.8
$Mg_4O(C_{3v}, II({}^1A_1))$	0	−873.145 53	112.9

[a] UHF/6-31G* was employed for open-shell species, RHF/6-31G* for closed-shell. The number of imaginary frequencies are given in parentheses.

set (HF/6-31G*)[37,38] and at correlated MP2(full) levels (UHF and UMP2 for open-shell systems). The results are summarized in Figure 1. Fundamental frequencies, normal coordinates, and zero-point energies (ZPE) were calculated by standard FG matrix methods. The MP2(full)/6-31G* equilibrium geometries were used to evaluate electron correlation in the frozen-core approximation both by Moller–Plesset perturbation theory to full fourth order[39] and by (U)QCISD(T)[40] methods using the 6-311+G* and 6-311+G(3df) basis sets. The UHF wave functions for open-shell systems were projected to pure spectroscopic states (PUHF, PMP2, PMP3, and PMP4).[41] Analytical frequencies at MP2(full)/6-31G* were carried out with the CADPAC program.[42] GAUSSIAN 90 (CONVEX version)[43] was used for the other calculations. The total energies at HF/6-31G* and at different correlated levels are presented in Tables I and II. Dissociation energies and harmonic frequencies are given in Tables III and IV, respectively. For estimation of the stability of the hypermagnesium molecules with respect to all possible dissociation pathways, reference data for the Mg(^{1}S) and O(^{3}P) atoms, as well as for the MgO ($^1\Sigma^+$, $^3\Pi$) molecule, were calculated. The total energies at HF/6-31G* and at different correlated levels using the 6-31G*, 6-311+G*, and 6-311+G(3df) basis sets are included in Tables I and II.

Results

MgO. The $^1\Sigma^+$ MgO ground state arises from the singlet coupling of the 3s electron of Mg^+ to the $p\sigma^1p\pi^4$ open shell of O^-. This state is not well represented by a single reference configuration, reflecting the fact that the charge distribution is intermediate between Mg^+O^- and $Mg^{2+}O^{2-}$.[22-25] Therefore, HF and correlated methods (like MP4) based on a single configuration reference state cannot be expected to give reasonable values for the dissociation energy. In the best available theoretical study, Langhoff et al.[25] estimated the dissociation energy of the $X^1\Sigma^+$ state of MgO indirectly by using the total energy of the $^3\Pi$ state of MgO, obtained at the CISD level with a large basis set $(12s9p12d6f/8s6p4d2f)_{Mg^+}$ $(11s7p9d3f/6s4p3d1f)_O$, and by correcting for the experimental $X^1\Sigma^+$–$a^3\Pi$ energy separation. The resulting D_e (MgO, $^1\Sigma^+$) is 63.4 kcal/mol.[25] The value of D_e(MgO, $^1\Sigma^+$) recommended by Huber and Herzberg[44] is 80.7 kcal/mol, which is a reinterpretation of the Srivastava resut,[31] taking into account the presence of the low-lying $^3\Pi$ state. However, Huber and Herzberg[44] pointed out that "the dissociation energy MgO (to Mg(^{1}S) + O(^{3}P)) is quite uncertain". Because our dissociation energies for MgO ($^1\Sigma^+$) oscillated along the MP2-MP3-MP4 series (see Table II), we estimated D_e of MgO ($^1\Sigma^+$) by employing the procedure of Langhoff et al. (see above).[25] We added the experimental $X^1\Sigma^+$–$a^3\Pi$ energy separation (0.326 eV[45]) to the total energies of MgO ($a^3\Pi$) calculated at QCISD(T)/6-311+G* and at QCISD(T)/6-311+G(3df) (both at optimized MP2(full)/6-31+G* geometry). The resulting D_e (MgO, $^1\Sigma^+$) is 58.8 kcal/mol at QCISD(T)/6-311+G(3df)+ZPE. We also used these estimated total energies of MgO ($^1\Sigma^+$) in our evaluations of the Mg_2O, Mg_3O, and Mg_4O dissociation energies, as discussed below.

Mg_2O. We have examined three Mg_2O forms at HF/6-31G*: linear Mg–O–Mg ($D_{\infty h}$), linear Mg–Mg–O ($C_{\infty v}$), and Mg–O–Mg (C_{2v}), all in singlet and triplet states (see Table I). The triplet $^3\Sigma_u^-$ linear Mg–O–Mg structure with a $(1\sigma_g)^2(1\sigma_u)^2(1\pi_u)^4(2\sigma_g)^1(2\sigma_u)^1(1\pi_g)^0$ valence configuration is an absolute minimum (no imaginary frequencies) at this level. Modest spin contamination ($\langle S^2 \rangle$ = 2.002) was found for the triplet linear structure at UHF. The linear singlet Mg–O–Mg structure $[(1\sigma_g)^2(1\sigma_u)^2(1\pi_u)^4(2\sigma_g)^2(2\sigma_u)^0$ configuration] is not a minimum and lies 46 kcal/mol above the ground state. Another linear singlet structure, Mg–Mg–O $[(1\sigma)^2(2\sigma)^2(1\pi)^4(3\sigma)^2(4\sigma)^2(2\pi)^0]$, is a local minimum (no imaginary frequencies), but is higher in energy than the dissociation products MgO($^1\Sigma^+$) + Mg(^{1}S).

Optimization of triplet C_{2v} Mg_2O leads to the linear $D_{\infty h}$ ($^3\Sigma_u^-$) ground-state configuration. The singlet C_{2v} structure of Mg_2O is a local minimum. But this structure is highly flexible (the barrier toward linearization is only 5.2 kcal/mol), and its relative energy is 41 kcal/mol. At this uncorrelated level, the stability of the Mg_2O forms is $D_{\infty h}(^3\Sigma_u^-) < C_{2v}(^1A_1) < D_{\infty h}(^1\Sigma_g^+) < C_{\infty v}(^1\Sigma^+)$.

The lowest energy linear triplet, linear singlet, and bent C_{2v} singlet structures of Mg_2O were reoptimized at the MP2(full)/6-31G* level, and single points were calculated at the QCISD(T)/6-311+G* and QCISD(T)/6-311+G(3df) levels. At our highest correlated levels MP4SDTQ/6-311+G(3df) and QCISD(T)/6-311+G(3df), the singlet linear $D_{\infty h}$ structure is the global minimum. The corresponding triplet structure is 4.6 and 3.5 kcal/mol higher in energy at the two levels, respectively. However, relative energies oscillated along the MP2-MP3-MP4 and QCISD-QCISD(T) series. Since the singlet state requires a multiconfiguration representation, we cannot predict which state is the more stable with certainty. However, both states of Mg_2O have similar energies and are stable toward dissociation. Optimization of the singlet C_{2v} structure at MP2(full)/6-31G* leads to the linear form; this behavior contrasts with that at HF/6-31G*.

We calculated the dissociation energy for the triplet state of $Mg_2O(^3\Sigma_u^-)$ into MgO($^3\Pi$) + Mg(^{1}S) to be 74.5 kcal/mol at QCISD(T)/6-311+G(3df)+ZPE. While the singlet states of MgO and Mg_2O require multiconfiguration descriptions, only small singlet–triplet splittings are expected in both molecules. Hence, the value of the dissociation energy of the triplet should be a reasonable estimate for the dissociation energy of Mg_2O ($^1\Sigma_g^+$) as well. The D_o of Mg_2O ($^1\Sigma_g^+$) was also estimated using the total energies of MgO ($^1\Sigma^+$) obtained as the sum of the total energy of MgO ($a^3\Pi$) and the experimental $X^1\Sigma^+$–$a^3\Pi$ energy separation. The D_o of Mg_2O ($^1\Sigma_g^+$), 77.0 kcal/mol, obtained in

(36) Schlegel, H. B. *J. Comput. Chem.* **1982**, *3*, 214.
(37) Hariharan, P. C.; Pople, J. A. *Theor. Chim. Acta* **1973**, *28*, 213.
(38) Frisch, M. J.; Pople, J. A.; Binkley, J. S. *J. Chem. Phys.* **1984**, *80*, 3265.
(39) Krishnan, R.; Pople, J. A. *Int. J. Quantum Chem.* **1978**, *14*, 91.
(40) Pople, J. A.; Head-Gordon, M.; Raghavachari, K. *J. Chem. Phys.* **1987**, *87*, 5968.
(41) Schlegel, H. B. *J. Chem. Phys.* **1986**, *84*, 4530.
(42) Amos, R. D.; Rice, J. E. *CADPAC: The Cambridge Analytic Derivatives Package*, Issue 4.0, Cambridge, England, 1987.
(43) GAUSSIAN 90 (CONVEX version): Frisch, M. J.; Head-Gordon, M.; Trucks, G. W.; Foresman, I. B.; Schlegel, H. B.; Raghavachari, K.; Robb, M. A.; Binkley, I. S.; Gonzales, C.; DeFrees, D. I.; Fox, D. I.; Whiteside, R. A.; Seeger, R.; Melius, C. F.; Baker, I.; Martin, R.; Kahn, L. R.; Stewart, I. I. P.; Fluder, E. M.; Topiol, S.; Pople, J. A. Gaussian Inc.: Pittsburgh, PA, 1990.
(44) Huber, K. P.; Herzberg, G. *Molecular Spectra and Molecular Structure*; van Nostrand Reinhold: New York, 1979.
(45) Ab initio Archive of the Institute of Organic Chemistry, Erlangen-Nürnberg University, unpublished results.

Table II. Calculated Correlated Absolute Energies E_t[a] of the Magnesium Oxide Species at the MP2(full)/6-31G* Geometries[b]

species structure state	UMP2 (full) 6-31G*	PMP2 6-311+G* 6-311+G(3df)	PMP3 6-311+G* 6-311+G(3df)	PMP4 6-311+G* 6-311+G(3df)	QCISD 6-311+G* 6-311+G(3df)	QCISD (T) 6-311+G* 6-311+G(3df)
$O(^3P)$	−74.882 00	−74.923 36	−74.935 43	−74.938 25	−74.936 75	−74.938 20
		−74.954 28	−74.968 09	−74.972 04	−74.968 90	−74.972 02
$Mg(^1S)$	−199.624 07	−199.628 65	−199.635 64	−199.638 18	−199.639 97	−199.639 97
		−199.629 88	−199.635 93	−199.638 27	−199.640 16	−199.640 16
$MgO(^1\Sigma^+)$	−274.600 99 (0)	−274.647 21	−274.604 45	−274.678 60	−274.641 52	−274.651 66
		−274.700 83	−274.659 00	−274.694 84	−274.688 21	−274.704 67
$MgO(^3\Pi)$	−274.585 52 (0)	−274.632 26	−274.638 02	−274.646 85	−274.642 83	−274.647 40
		−274.678 49	−274.686 29	−274.696 09	−274.688 95	−274.696 01
$Mg_2O(D_{\infty h}, {}^3\Sigma_u^-)$	−474.341 40 (0)	−474.389 41	−474.375 28	−474.400 79	−474.388 25	−474.396 81
		−474.447 99	−474.435 65	−474.461 71	−474.444 43	−474.456 81
$Mg_2O(D_{\infty h}, {}^1\Sigma_g^+)$	−474.328 02 (0)	−474.374 28	−474.367 40	−474.410 01	−474.383 84	−474.402 53
		−474.433 87	−474.426 52	−474.469 08	−474.438 70	−474.462 31
$Mg_3O(C_{2v}, I(^1A_1))$	−673.974 71 (0)	−674.023 54	−674.022 95	−674.057 91	−674.042 76	−674.059 46
$Mg_3O(C_{2v}, II(^1A_1))$	−673.988 88 (0)	−674.035 99	−674.035 87	−674.069 27	−674.052 78	−674.069 83
$Mg_3O(D_{3h}, {}^3A_1')$	−674.009 69 (0)	−674.061 73	−674.055 04	−674.083 98	−674.068 98	−674.081 59
$Mg_4O(C_{2v}, I(^3A_1))$	−873.623 06 (0)	−873.682 13	−873.682 16	−873.712 65		
$Mg_4O(C_{2v}, I(^1A_1))$	−873.640 88 (2)	−873.691 92	−873.697 80	−873.734 51		
$Mg_4O(D_{4h}, {}^1A_{1g})$	−873.641 52 (1)	−873.688 84	−873.695 63	−873.730 62		
$Mg_4O(C_s, {}^1A')$	−873.642 01 (0)	−873.692 60	−873.698 35	−873.734 74		
$Mg_4O(D_{2d}, {}^1A_1)$	−873.643 18 (0)	−873.690 50	−873.697 78	−873.732 57		

[a] The energies are given in au. [b] The number of imaginary frequencies are given in parentheses.

this way does not differ much from the D_0 value given above. Taking the singlet–triplet splitting into account, we suggest D_0-(MgO–Mg) for $MgO(^1\Sigma^+)$ + Mg to be 75 ± 10 kcal/mol. This is even higher than our value for the dissociation energy of MgO ($^1\Sigma^+$). Hence, the Mg_2O molecule should be a viable species in isolation.

Mg_3O. The canonical order of the AX_3 MOs in Figure 2 suggests that the D_{3h} structure of Mg_3O should be a triplet (12 valence electrons). The C_{2v},I or C_{2v},II Mg_3O singlet geometries (Figure 1, middle) arise from Jahn–Teller distortion of the singlet D_{3h} structure (two electrons in an e MO). We have examined five basic forms of Mg_3O: at HF/6-31G* and MP2(full)/6-31G* D_{3h}, C_{2v},I, C_{2v},II, C_{2v},III, C_{2v},III, and C_{3v}, all in singlet and triplet states (see Table I). At the MP2(full)/6-31G* correlated level, both C_{2v},I($^3B_2$) and C_{2v},II($^3B_2$) forms collapse into the $D_{3h}(^3A_1)$ structure, which is an absolute minimum at all correlated levels.

Our best estimate for the dissociation energy of Mg_3O (D_{3h}, $^3A_1'$) into $Mg_2O(D_{\infty h}, {}^3\Sigma_u^-)$ + Mg(^{1}S) is 26.7 kcal/mol at QCISD(T)/6-311+G*. Taking the singlet–triplet splitting in Mg_2O into account, we suggest D_0 for Mg_3O into Mg_2O + Mg to be 25 ± 10 kcal/mol. Mg_3O also should be a viable species, stable toward all possible modes of dissociation. Our calculated frequencies at MP2(full)/6-31G* may help identification of the Mg_3O molecule in matrix isolation and in the gas phase.

Mg_4O. Our preliminary search of various Mg_4O geometries at HF/6-31G* included the T_d, D_{4h}, D_{2d}, C_{2v},I, C_{2v},II, C_{3v},I, and C_{3v},II structures in the triplet and singlet states. The lowest energy C_{2v},I($^3B_2$), C_{2v},I($^1A_1$), $C_s(^1A')$, $D_{4h}(^1A_{1g})$, and $D_{2d}(^1A_1)$ structures were reoptimized at MP2(full)/6-31G*.

The singlet T_d geometry of Mg_4O is not expected to be stable toward Jahn–Teller distortion, because only four electrons are available to occupy the t_2 HOMO [$(1a_1)^2(1t_2)^6(2a_1)^2(2t_2)^4(1e)^0$ valence configuration]. Distortion points toward the D_{4h} planar geometry. According to the canonical MO order for MX_4 (Figure 3), singlet Mg_4O might possess a $^1A_1{}^g$ ground state in D_{4h} symmetry [$(1a_{1g})^2(1e_u)^4(1a_{2u})^2(2a_{1g})^2(2e_u)^4(1b_{1g})^0$ configuration]. The doubly-degenerate $2e_u$ HOMO would then be completely occupied. In the triplet state, the D_{4h} geometry ($(2e_u)^3(1b_{1g})^1$) should be unstable toward Jahn–Teller distortion. However, D_{4h} symmetry for singlet Mg_4O is not favored at either the uncorrelated HF/6-31G* or at the correlated MP2(full)/6-31* level. At both, the D_{4h} structure is a saddle point. The instability of the D_{4h} geometry is due to the relatively short Mg–Mg distances (R(Mg–Mg) = 2.817 Å in Mg_4O (D_{4h}, $^1A_1$) vs R(Mg–Mg) = 2.912 Å in HMg–MgH at HF/6-31G*[46]). The vector of the imaginary frequency in the D_{4h} structure leads to D_{2d} symmetry. Indeed, optimization in D_{2d} symmetry leads to the slightly deformed square planar D_{2d} structure [$^1A_1$; $(1a_1)^2(1e)^4(1b_2)^2(2a_1)^2(2e)^4(2b_2)^0$ valence configuration]. The O–Mg bonds deviate 15° from the plane; R(Mg–Mg) = 2.917 Å, which is close to R(Mg–Mg) in HMgMgH (see above). This D_{2d} structure of Mg_4O is a local minimum at HF/6-31G* and is the global minimum at the

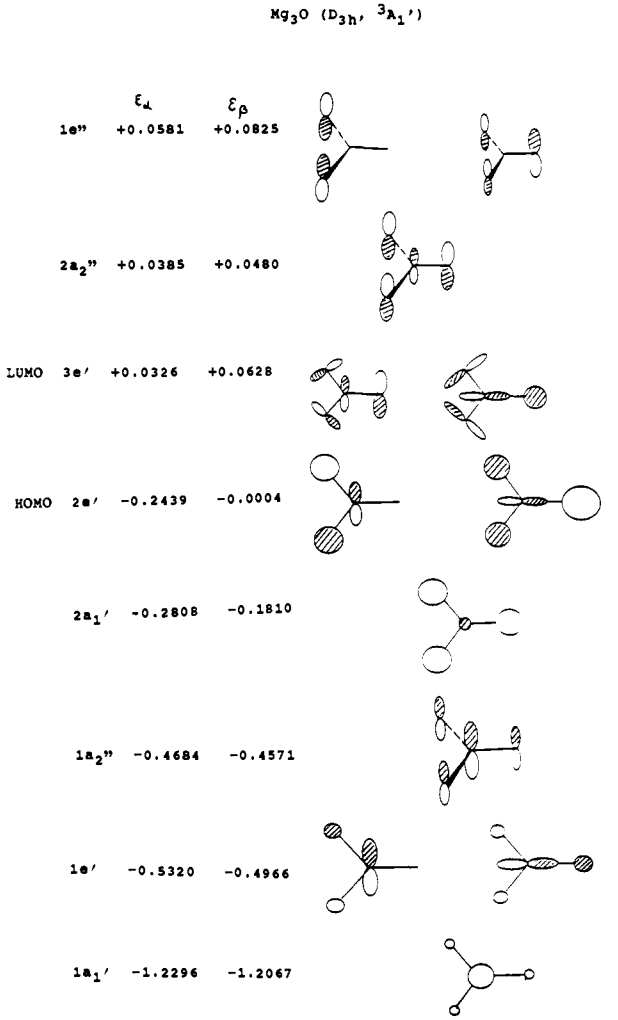

Figure 2. MO scheme of Mg_3O (D_{3h}, $^3A_1'$).

(46) Reed, A. E.; Weinhold, F. *QCPE Bull.* **1985**, *5*, 141.

Table III. Calculated Dissociation Energies of the Magnesium Oxide Species[a]

reaction	MP2(full) 6-31G*	PMP2 6-311+G* 6-311+G(3df)	PMP3 6-311+G* 6-311+G(3df)	PMP4 6-311+G* 6-311+G(3df)	QCISD(T) 6-311+G* 6-311+G(3df)	QCISD(T) + ZPE 6-311+G* 6-311+G(3df)
$MgO(^3\Pi) \rightarrow Mg + O$	+49.9	+50.4	+42.0	+44.2	+43.4	+42.5
		+59.2	+51.6	+53.8	+52.6	+51.7
$Mg_2O(^3\Sigma_u^-) \rightarrow MgO(^3\Pi) + Mg$	+82.7	+80.6	+63.8	+72.6	+68.7	+67.5
		+87.6	+71.2	+79.2	+75.7	+74.5
$Mg_2O(^3\Sigma_u^-) \rightarrow O + 2Mg$	+132.6	+131.0	+105.8	+116.8	+112.1	+110.0
		+146.8	+122.8	+133.7	+128.3	+126.2
$Mg_3O(^3A_1') \rightarrow Mg_2O(^3\Sigma_u^-) + Mg$	+27.7	+27.4	+27.7	+28.2	+28.1	+26.7
$Mg_3O(^3A_1') \rightarrow MgO(^3\Pi) + 2Mg$	+110.5	+108.0	+91.5	+100.9	+96.8	+94.2
$Mg_3O(^3A_1') \rightarrow O + 3Mg$	+160.3	+158.4	+133.5	+145.0	+140.2	+136.7
$Mg_4O(^1A') \rightarrow Mg_3O(^3A_1') + Mg$	+5.2	+1.4	+4.8	+7.9		+7.9[b]
$Mg_4O(^1A') \rightarrow Mg_2O(^3\Sigma_u^-) + 2Mg$	+32.9	+28.8	+32.5	+35.1		
$Mg_4O(^1A') \rightarrow MgO(^3\Pi) + 3Mg$	+115.6	+109.4	+96.3	+108.8		
$Mg_4O(^1A') \rightarrow O + 4Mg$	+165.5	+159.8	+138.3	+153.0		

[a] The energies are given in kcal/mol. [b] At PMP4SDTQ/6-311+G*+ZPE//MP2(full)/6-31G*.

Table IV. Calculated Harmonic Frequencies (cm^{-1}) and IR Intensities (in parentheses, KM/mol) of the Magnesium Oxides

spec, sym	freq	HF/ 6-31G*	MP2(full)/ 6-31G*	spec, sym	freq	HF/ 6-31G*	MP2(full)/ 6-31G*	spec, sym	freq	HF/ 6-31G*	MP2(full)/ 6-31G*
$MgO(^1\Sigma^+)$	ω_e		915	$Mg_3O(C_{2v}, I(^3B_2))$	$\nu_1(a_1)$	756 (126)		$Mg_4O(C_s, {}^1A')$	$\nu_1(a')$	701 (19)	
	ZPE		1.3		$\nu_2(a_1)$	421 (0)			$\nu_2(a')$	552 (15)	
$MgO(^3\Pi)$	ω_e		655		$\nu_3(a_1)$	193 (4)			$\nu_3(a')$	417 (4)	
	ZPE		0.9		$\nu_4(b_1)$	144 (4)			$\nu_4(a')$	248 (118)	
$Mg_2O(D_{\infty h}, {}^3\Sigma_u^-)$	$\nu_1(\sigma_g)$	519 (0)	476 (0)		$\nu_5(b_2)$	506 (49)			$\nu_5(a')$	207 (37)	
	$\nu_2(\Pi_u)$	98 (10)	46 (7)		$\nu_6(b_2)$	130 (5)			$\nu_6(a')$	165 (32)	
	$\nu_3(\sigma_u)$	981 (392)	905 (318)		ZPE	3.1			$\nu_7(a'')$	117 (22)	
	ZPE	2.4	2.1	$Mg_3O(C_{2v}, II(^3B_2))$	$\nu_1(a_1)$	562			$\nu_8(a'')$	166 (4)	
$Mg_2O(C_{2v}, {}^1A_1)$	$\nu_1(a_1)$	723 (66)			$\nu_2(a_1)$	416			$\nu_9(a'')$	53 (2)	
	$\nu_2(a_1)$	183 (9)			$\nu_3(a_1)$	100			ZPE	3.8	
	$\nu_3(b_2)$	758 (110)			$\nu_4(b_1)$	112		$Mg_4O(D_{2d}, {}^1A_1)$	$\nu_1(a_1)$	379 (0)	354 (0)
	ZPE	2.4			$\nu_5(b_2)$	386			$\nu_2(a_1)$	69 (0)	58 (0)
$Mg_2O(D_{\infty h}, {}^1\Sigma_g^+)$	$\nu_1(\sigma_g)$	508	466 (0)		$\nu_6(b_2)$	2068i			$\nu_3(b_1)$	203 (0)	187 (0)
	$\nu_2(\Pi_u)$	83i	86 (26)		ZPE	2.3			$\nu_4(b_2)$	284 (14)	287 (5)
	$\nu_3(\sigma_u)$	916	881 (285)	$Mg_4O(D_{4h}, {}^1A_{1g})$	$\nu_1(a_{1g})$	379	358		$\nu_5(b_2)$	134 (37)	94 (19)
	ZPE	2.0	2.2		$\nu_2(a_{2u})$	149	102		$\nu_6(e)$	474 (21)	458 (31)
$Mg_2O(C_{\infty v}, {}^1\Sigma^+)$	$\nu_1(\sigma)$	889 (13)			$\nu_3(b_{1g})$	224	220		$\nu_7(e)$	42 (11)	174 (4)
	$\nu_2(\sigma)$	135 (14)			$\nu_4(b_{2g})$	239	225		ZPE	3.0	3.2
	$\nu_3(\Pi)$	54 (46)			$\nu_5(b_{2u})$	60i	55i	$Mg_4O(C_{2v}, I(^1A_1))$	$\nu_1(a_1)$	642	650
	ZPE	1.6			$\nu_6(e_u)$	450	439		$\nu_2(a_1)$	420	387
$Mg_3O(D_{3h}, {}^3A_1)$	$\nu_1(a_1')$	415	387 (0)		$\nu_7(e_u)$	58	198		$\nu_3(a_1)$	253	191
	$\nu_2(a_2'')$	111	110 (0)		ZPE	2.8	3.1		$\nu_4(a_1)$	133	105
	$\nu_3(e')$	551	777 (5120)	$Mg_4O(C_{2v}, I(^3A_1))$	$\nu_1(a_1)$	711 (105)	684 (95)		$\nu_5(b_1)$	144	105
	$\nu_4(e')$	156i	205 (316)		$\nu_2(a_1)$	392 (3)	362 (0)		$\nu_6(b_1)$	24	50i
	ZPE	2.3	3.5		$\nu_3(a_1)$	226 (3)	233 (4)		$\nu_7(b_2)$	647	575
$Mg_3O(C_{2v}, I(^1A_1))$	$\nu_1(a_1)$	724 (125)	643 (36)		$\nu_4(a_1)$	144 (4)	117 (7)		$\nu_8(b_2)$	230	182
	$\nu_2(a_1)$	367 (0)	309 (5)		$\nu_5(b_1)$	181 (6)	149 (2)		$\nu_9(b_2)$	86i	67i
	$\nu_3(a_1)$	225 (30)	120 (10)		$\nu_6(b_1)$	46 (2)	42 (2)		ZPE	3.6	3.2
	$\nu_4(b_1)$	84 (12)	24 (2)		$\nu_7(b_2)$	542 (5)	471 (28)	$Mg_4O(C_s, {}^1A')$	$\nu_1(a')$	701 (19)	662
	$\nu_5(b_2)$	621 (60)	629 (10)		$\nu_8(b_2)$	166 (27)	166 (58)		$\nu_2(a')$	552 (15)	551
	$\nu_6(b_2)$	253 (64)	102 (30)		$\nu_9(b_2)$	121 (1)	106 (0)		$\nu_3(a')$	417 (4)	387
	ZPE	3.3	2.6		ZPE	3.6	3.3		$\nu_4(a')$	248 (118)	237
$Mg_3O(C_{2v}$, $II(^1A_1))$	$\nu_1(a_1)$	586 (3)	550	$Mg_4O(C_{2v}, I(^1A_1))$	$\nu_1(a_1)$	642	650		$\nu_5(a')$	207 (37)	194
					$\nu_2(a_1)$	420	387		$\nu_6(a')$	165 (32)	144
	$\nu_2(a_1)$	397 (27)	367		$\nu_3(a_1)$	254	191		$\nu_7(a')$	117 (22)	97
	$\nu_3(a_1)$	178 (18)	138		$\nu_4(a_1)$	133	122		$\nu_8(a'')$	166 (4)	127
	$\nu_4(b_1)$	105 (9)	66		$\nu_5(b_1)$	144	105		$\nu_9(a'')$	53 (2)	24
	$\nu_5(b_2)$	702 (17)	636		$\nu_6(b_1)$	24	50i		ZPE	3.8	3.5
	$\nu_6(b_2)$	222 (234)	215		$\nu_7(b_2)$	647	575				
	ZPE	3.1	2.8		$\nu_8(b_2)$	231	182				
$Mg_3O(C_{2v}$, $III(^1A_1))$	$\nu_1(a_1)$	616 (49)			$\nu_9(b_2)$	86i	67i				
					ZPE	3.6	3.2				
	$\nu_2(a_1)$	285 (11)									
	$\nu_3(a_1)$	63 (46)									
	$\nu_4(b_1)$	156 (9)									
	$\nu_5(b_2)$	803 (69)									
	$\nu_6(b_2)$	237 (51)									
	ZPE	3.1									

MP2(full)/6-31G* level (see Tables I and II). The $D_{2d}(^1A_1)$ structure is very flexible. The barrier toward inversion through the planar D_{4h} structure is only 1.2 kcal/mol (MP4SDTQ/6-311+G*//MP2(full)/6-31G*). The dissociation energy of Mg_4O (D_{2d}, $^1A_1$) into $Mg_3O(D_{3h}, {}^3A_1') + Mg(^1S)$ is only 7.9 kcal/mol at our highest MP4SDTQ/6-311+G* level.

The two C_{2v} structures of Mg_4O (in which an MgO unit is coordinated via the oxygen atom to the edge (C_{2v},I) and to the vertex (C_{2v},II) of triangular Mg_3; see Figure 1) were examined in the singlet and triplet states. The C_v,$I(^3B_2)$ structure is a local minimum at MP2(full)/6-31G* with a relative energy of 11.6 kcal/mol vs the $D_{2d}(^1A_1)$ form (see Tables I and II). The singlet C_{2v},$I(^1A_1)$ structure is a second-order saddle point (two imaginary frequencies) at MP2(full)/6-31G* with a relative energy of 1.5 kcal/mol. Moreover, at MP4SDTQ/6-311+G*, the C_{2v},$I(^1A_1)$ configuration is even lower in energy than the D_{2d} structure. The vector of the imaginary frequency of the C_{2v},$I(^1A_1)$ structure leads to the planar $C_s(^1A')$ form. The Mg_b–Mg_t separations in the $C_{2v}(^1A_1)$ configuration of Mg_4O are too large (3.302 Å) with respect to the optimal Mg–Mg distance, 2.9 Å. Therefore, in the $C_s(^1A')$ structure, the terminal Mg moves toward the bridging Mg atom (the Mg_b–Mg_t separation is 2.901 Å). This C_s form

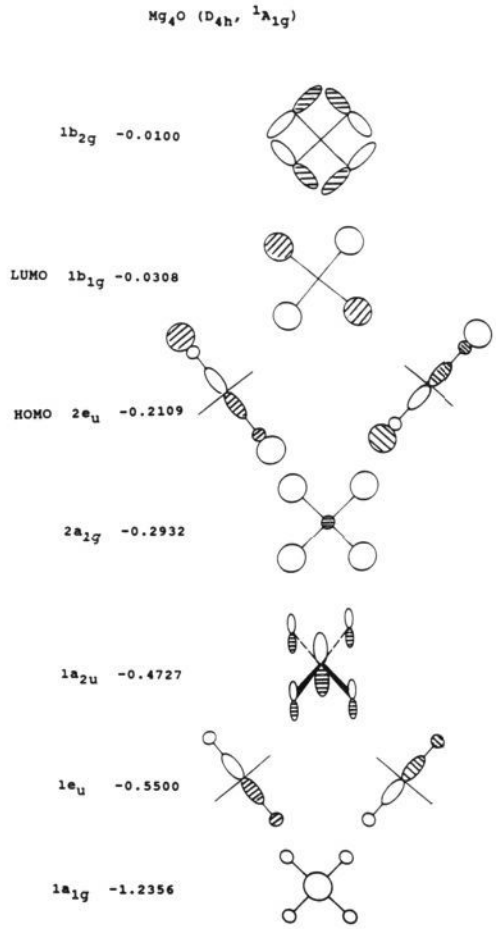

Figure 3. MO scheme of Mg_4O (D_{2d}, $^1A_1$).

is a second minimum at MP2(full)/6-31G* lying only 0.7 kcal/mol higher than the D_{2d} structure, but is the most stable geometry at our highest (MP4SDTQ/6-311+G*) level. However, the energy difference between the singlet D_{2d} and C_s minima is not high, only 1.4 kcal/mol. Both forms may coexist in matrix isolation. The dissociation energy of $Mg_4O(C_s, {}^1A')$ into $Mg_3O(D_{3h}, {}^3A_1')$ + $Mg(^1S)$ is 7.9 kcal/mol at PMP4SDTQ/6-311+G*. Therefore, both the D_{2d} and C_s structures of Mg_4O are not very stable thermodynamically, especially when the contribution of dissociation entropies is taken into consideration.

Since the two C_{3v} structures were quite high in energy, they were not studied further at correlated levels.

Bonding and Structure of the Magnesium Oxides

We wish to comment on the wave functions of the systems under consideration, because our computational formalisms apply to states which are well represented by Hartree–Fock functions. Information on multiconfigurational contribution can be obtained from the coefficients of the CASSCF or the QCISD expansion. The geometries both of singlet ($^1\Sigma_g^+$) and triplet ($^3\Sigma_u^-$) electronic states of Mg_2O were optimized with the 6-31G* basis set at the CASSCF(2,2), CASSCF(2,4), CASSCF(2,6), and CASSCF(4,6) levels (the numbers in parentheses designate the number of active electrons and the number of active MOs, in that order). The total energy of the singlet state of Mg_2O changes considerably from HF(−474.026 31 au) to CASSCF(2,2) (−474.102 61 au), but using more active electrons and more MOs does not change the total energy very much of the singlet state of Mg_2O at CASSCF(4,6) (−474.117 78 au). Hence, singlet Mg_2O is mainly a two-determinant state (the largest coefficients are 0.77 and −0.63, respectively, at $(1\sigma_g)^2(1\sigma_u)^2(1\pi_u)^4(2\sigma_g)^2(2\sigma_u)^0$ and $(1\sigma_g)^2(1\sigma_u)^2(1\pi_u)^4(2\sigma_u)^2(2\sigma_g)^0$). The other coefficients are smaller than 0.02 in the CASSCF(4,6) expansion. The large contribution from the $(2\sigma_u)^2$ configuration is due to the biradical character of singlet Mg_2O. The two electrons involved prefer to localize at the Mg

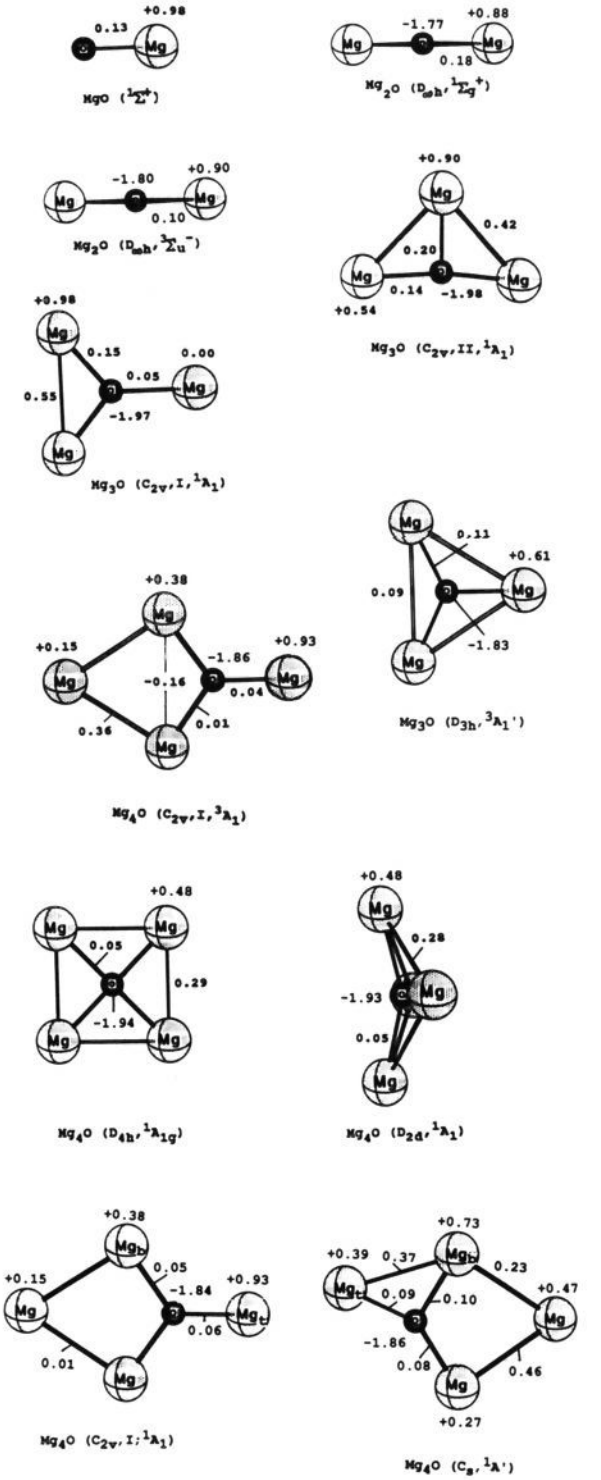

Figure 4. Natural charges and atom–atom overlap-weighted NAO bond orders of magnesium oxides.

atoms. However, triplet Mg_2O is mainly a one-determinant state (the coefficient is higher than 0.99 in the $(1\sigma_g)^2(1\sigma_u)^2(1\pi_u)^4(2\sigma_g)^1(2\sigma_u)^1$ HF configuration with CASSCF(4,6)). Hence, our triplet-state calculations of Mg_2O at the MP2 and QCISD(T) levels should be appropriate. For other species (MgO, Mg_3O, and Mg_4O), we may use QCISD expansions to estimate multiconfigurational contributions. According to these data, several configurations contribute to the wave functions of singlet MgO, Mg_2O, and Mg_3O. The largest coefficients are 0.76 (MgO), 0.61 (Mg_2O), 0.22 (Mg_3O,I), and 0.07 (Mg_3O,II). However, in triplet states of MgO ($^3\Pi$), Mg_2O ($^3\Sigma_u^-$), and Mg_3O ($^3A_1'$), the largest coefficients from the non-Hartree–Fock configurations are quite small (<0.045). Therefore the triplet states are quite well rep-

resented by unrestricted Hartree-Fock wave functions, and our calculated dissociation energies should be reasonable estimates (±10 kcal/mol) for these species.

Natural population and natural bond orbital analyses[47,48] of the various magnesium oxide species are summarized in Figure 4.

In both singlet and triplet states of MgO, the oxygen charges are close to −1.0. Hence, representations like Mg=O are inappropriate. Singlet-triplet splitting is small (0.326 eV),[32] and the covalent coupling of the second pair of electrons is very weak. This weak coupling of the second pair of electrons allows MgO to bind an additional Mg atom to give the linear Mg-O-Mg molecule. The oxygen and magnesium charges in Mg-O-Mg are quite close to −2.0 and +1.0, respectively (at HF/6-311+G*). Hence, the charge distribution is similar to that in Na_2O. The two extra electrons in Mg_2O (vs Na_2O) are located on the Mg atoms. Coupling of these two electrons is also very weak (the singlet-triplet splitting is 0.15 eV at QCISD(T)/6-311+G(3df)). Both MgO and Mg_2O may be represented approximately as $Mg^{1+}O^{1-}$ and $Mg^{1+}O^{2-}Mg^{1+}$. Therefore, a linear geometry is expected for Mg_2O on the basis of electrostatics. The dissociation energies increase in going from MgO (51.7 kcal/mol) to Mg_2O (74.5 kcal/mol (QCISD(T)/6-311+G(3df)+ZPE). The structure and stability of the hyperstoichiometric Mg_2O molecule are largely due to the ionic nature of the bonding.

Bonding Mg-Mg interactions do contribute to the stability of Mg_3O. However, due to the low energy of the Mg-Mg bond, the dissociation energy of Mg_3O (into Mg_2O + Mg) is only 26.7 kcal/mol at QCISD(T)/6-311+G*+ZPE. This value is quite close to the dissociation energy of Al_3O (into Al_2O + Al) (19.9 kcal/mol at PMP4SDTQ/6-311+G*), where metal-metal interactions contribute to the stability.[20] While the ligand-ligand overlap population is even larger in the case of Mg_4O (D_{2d}, $^1A_1$), the Mg-Mg distances are forced to be too short. This leads to increased ligand-ligand electrostatic repulsion. Hence, the dissociation energy of Mg_4O (D_{2d}, $^1A_1$) into Mg_3O + Mg is quite low. In contrast, Al_4O (D_{4h}, A_{1g}) is very stable.[20] The Al-Al bond distance in square planar Al_4O is close to the optimum value (e.g., as in H_2AlAlH_2).[45]

(47) Reed, A. E.; Weinhold, F. *Chem. Rev.* **1988**, *88*, 889.
(48) Lammertsma, K.; Güner, O. F.; Drewes, R. M.; Reed, A. E.; Schleyer, P. v. R. *Inorg. Chem.* **1989**, *28*, 313.

Conclusions

The main conclusions of this study are the following: (1) The hypermagnesium Mg_2O, Mg_3O, and Mg_4O molecules are stable toward all possible dissociation modes. However, in contrast to Mg_2O and Mg_3O, the dissociation energy of Mg_4O into Mg_3O and Mg is low. Mg_2O (both in the singlet and triplet states) and Mg_3O (triplet) prefer linear and planar triangular geometries, respectively. Mg_4O favors a structure only slightly distorted from planarity (D_{2d}) as well as a planar $MgOMg_3$ (C_s) singlet. Several additional Mg_3O and Mg_4O singlet and triplet minima are possible. (2) The high degree of $Mg^{0.5-0.7+}O^{2-}$ ionic character as well as Mg-Mg bonding are responsible for the stability of the hypermetalated Mg_3O and Mg_4O species. However, the hyperstoichiometric Mg_2O molecule may be represented classically as $Mg^{1+}O^{2-}Mg^{1+}$.

Acknowledgment. This work was facilitated by an Alexander-von-Humboldt Fellowship to A.I.B. and was supported by the Fonds der Chemischen Industrie, the Stiftung Volkswagenwerk, the Deutsche Forschungsgemeinschaft, and the Convex Computer Corporation.

Registry No. Mg_2O, 12201-41-1; Mg_3O, 141753-82-4; Mg_4O, 141753-83-5.

Theoretical Investigation of the Geometric Structures and the Second-Order Nonlinear Optical Properties of 8-Hydroxyquinoline Derivatives

Mamoun M. Bader,*,† Tomoyuki Hamada, and Atsushi Kakuta

Contribution from Hitachi Research Laboratory, Hitachi Ltd., Hitachi City, Ibaraki 319-12, Japan. *Received September 4, 1991*

Abstract: We report here the coupled perturbed Hartree-Fock (CPHF) ab initio extended basis set calculations on the geometric structures and static first-order (α) and second-order (β) polarizabilities of a series of 8-hydroxyquinoline molecules substituted by fluoro, chloro, nitro, and amino groups. Twenty one compounds were investigated in this study by considering the basis set dependence of the molecular hyperpolarizabilities. The effects of the nature and the position of the substituent on the geometry and the first-order and second-order polarizabilities are described. 2-Amino-6-nitro-8-quinolinol is calculated to have a β_{vec} of 14.739×10^{-30} esu which is almost twice as large as that for *p*-nitroaniline. On the basis of these calculations, new trends for the molecular design of fused heterocyclic aromatic compounds for second-order nonlinear optical applications are proposed.

I. Introduction

The discovery that conjugated organic materials exhibit large optical nonlinearities has triggered large-scale theoretical and experimental investigations in this area.[1-4] The identification of new materials with large nonlinear optical properties has many potential applications in a variety of laser-related technologies.[4] Since most organic materials form molecular crystals in which the molecules are held by weak van der Waals interactions, their

† Current address: Department of Chemical Engineering and Materials Science, University of Minnesota, Amundson Hall, 421 Washington Ave. S. E., Minneapolis, MN 55414.

(1) Chemla, D. S.; Zyss, J., Eds. *Nonlinear Optical Properties of Organic Molecules and Crystals*; Academic Press: New York, 1987; Vols. 1 and 2.
(2) Heeger, A. J.; Orenstein, J.; Ulrich, D. R., Eds. *Nonlinear Optical Properties of Polymers*: Materials Research Society Symposium Proceedings, Boston, MA, 1988; Vol. 109.
(3) Chiang, L. Y.; Chaikin, P. M.; Cowan, D. O., Eds. *Advanced Organic Solid State Materials*: Materials Research Society Symposium Proceedings, Boston, MA, 1990; Vol. 173.

0002-7863/92/1514-6475$03.00/0